

Network Decomposition via Graph Theory

Seth Blumsack

Abstract—In this paper, we provide a graph-theoretic heuristic algorithm for decomposing generic networks into series-parallel components and components representing embedded Wheatstone sub-networks. The decomposition algorithm is illustrated in detail on a thirteen-bus network. A network equivalencing method based on the delta-star and Ward equivalents is presented for use in power systems analysis.

Index Terms—Graph Theory, Braess Paradox, Diakoptics, Network Decomposition

I. INTRODUCTION

Graph theory and network theory have been surprisingly little-used tools in the analysis of power systems. However, in the context of transmission planning and congestion management, knowledge of the electric grid’s topological properties can be valuable, particularly with respect to the behavior of locational marginal prices (LMP) in market-based electric systems, and the possible congestion and reliability consequences of transmission upgrades in more traditionally-organized systems.

Recent work [1], [2] has focused on a particular network topology known as the Wheatstone network. This structure resembles two back-to-back triangles, and is shown in Figure 1. The link connecting nodes 2 and 3 is of particular interest; this is known as the Wheatstone bridge. When the direction of flow through the Wheatstone network is similar to the example network in Figure 1, the presence of the Wheatstone bridge causes congestion. Removal of the bridge removes the congestion. This phenomenon is known as the Braess Paradox, and has been observed in many different types of networks, ranging from circuits to water pipes ([4] – [6]). [2] focuses on power networks specifically.

In systems using locational marginal pricing to manage congestion in an open-access transmission environment, the presence of an embedded Wheatstone sub-network may affect how these prices should be interpreted. The LMPs represent the system marginal cost of supplying power to a given bus in the network; LMP differences between buses i and j should

measure the system cost of transferring power between those two buses, and the associated value of additional transmission capacity between those two buses. However, in the Wheatstone network studied in Blumsack and Ilić (2006) exposes a possible wedge between the pricing signals and the physical state of the network. LMPs indicate that localized transmission upgrades should relieve congestion and lower prices at downstream nodes. Attaining this goal in the Wheatstone network requires either upgrading transmission capacity across the entire network, or removing the Wheatstone bridge.

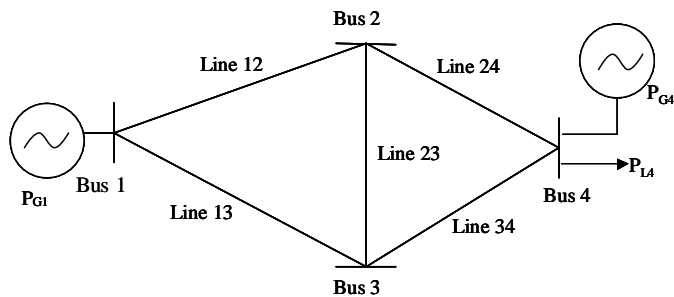


Figure 1. The four-bus Wheatstone network.

The Wheatstone network also exposes potential tradeoffs between congestion and reliability. While the Wheatstone bridge causes congestion and increases the cost to customers on the network, it may enhance reliability and therefore provide a benefit to that same group of consumers [7].

Thus, for both planning and congestion-management purposes, there may be value in knowing the location of embedded Wheatstone sub-networks. This paper proposes a heuristic search algorithm which identifies embedded Wheatstone sub-networks by exploiting some of their unique graph-theoretic properties. The algorithm interprets the electric grid as a generic graph, looking solely for Wheatstone topologies. In this way, the approach taken here has less in common with the diakoptics approach pioneered by Gabriel Kron and Henry Happ [8], [9], and much more in common with the series-parallel network decompositions of [10] and [11]. Following the description of the Wheatstone search algorithm and an example on a small test network, the paper discusses network equivalencing techniques that can be used to analyze embedded Wheatstone sub-networks while incorporating information from other parts of the network.

This work was funded by a grant to the Carnegie Mellon Electricity Industry Center from EPRI and the Alfred P. Sloan foundation. Any opinions and errors are those of the authors and should not be ascribed to the grantors.

II. A GRAPH-THEORETIC APPROACH TO NETWORK SEARCH

Wheatstone network structures are ubiquitous in actual power networks. In small test networks, visual inspection may be sufficient to identify all embedded Wheatstone sub-networks. In actual power systems, which may consist of thousands of nodes and even more lines, a more systematic approach is needed.

A purely combinatorial approach to finding embedded Wheatstone structures is possible on extremely small scales, but quickly becomes infeasible as the number of nodes increases. On a topological basis alone, comparing all four-node substructures of an n -bus network requires checking 4^n different combinations. To find all Wheatstone networks in the IEEE 14-bus network by brute force would therefore require 2.7×10^8 calculations. Checking for Wheatstones in the IEEE 118-bus network would require approximately 10^{71} calculations. By comparison, the approximate number of seconds since the beginning of the universe is only 3×10^{17} .

Designing a feasible algorithm for detecting Wheatstone sub-networks is essentially an application of the theorems in [10], also proved in [11], that any network can be decomposed into series-parallel sub-networks and embedded Wheatstone sub-networks. The decomposition problem is to break the network into portions that might represent Wheatstones, and portions that definitely do not. From a graph-theoretic perspective, electric power systems are nice test-beds for decomposition algorithms, since they tend to be very sparsely connected, with a given bus attached to a reasonably small number of other buses.

Some preliminaries are necessary before defining any specific metrics. A *graph* or a *network* $G(NB, NL)$ is defined as a set of nodes NB and a set of edges NL connecting the nodes. While complex networks often assume the existence of *hyper-edges* connecting more than two nodes (Newman 2003), an edge in this analysis will be assumed to connect only two nodes. A *path* is a sequence of nodes $\{i_1, i_2, \dots, j\}$, all of which are connected by edges; in many circumstances, paths will be denoted only by their endpoints i and j .

Connectivity in a graph or network is described using incidence matrices. The $(NB \times NB)$ node-node incidence matrix, denoted \mathbf{N} , shows which nodes in the network are connected neighbors; that is, which nodes are connected by a path of length one. The (i, j) th entry of \mathbf{N} is equal to one if node i is a connected neighbor of node j , and is equal to zero otherwise. If $N_{ij} = 1$, then network flow is possible from node i to node j . A graph is said to be *undirected* if \mathbf{N} is symmetric. DC power networks, or networks equipped with flow-control devices such as phase-angle regulators or voltage regulators, could be described as *directed* networks, where it is not necessarily true that $N_{ij} = N_{ji}$. The current U.S. high-voltage transmission grid represents a mix of AC and DC interconnections, with very few flow-control devices. Thus, representing the transmission system as an undirected network is a reasonable approximation of the current system.

We also define a node-edge (or node-line, in the context of power systems) adjacency matrix. Denoted as \mathbf{A} , the node-edge adjacency matrix is an $(NB \times NL)$ matrix with $a_{li} = +1$ and $a_{lj} = -1$, signifying that edge l connects nodes i and j . The sign of the entries in the \mathbf{A} matrix indicates an assumed direction of flow throughout the network (that is, from node i to node j). The principle of superposition says that either sign convention is appropriate, as long as it is consistent.

\mathbf{N} and \mathbf{A} are assumed to have the following properties:

1. $\forall j, \sum_i a_{ij} = 0$. This is just an application of Kirchoff's Law; it says that every link in the system connects exactly two nodes.
2. There are no columns of \mathbf{A} containing all zeros. In other words, there are no loops in the system.
3. There are no rows or columns of \mathbf{N} containing all zeros. In other words, there are no atomistic nodes or sub-systems in the network; each node is connected to at least one other node.
4. $\text{rank}(\mathbf{A}) = NL - 1$. This is a consequence of Euler's formula, which says that (nodes) – (edges) + (loops) = 1.
5. \mathbf{N} and \mathbf{A} are related by the formula $\mathbf{N} = \mathbf{A}\mathbf{A}' - 2\mathbf{I}$, where \mathbf{I} is the $(NB \times NB)$ identity matrix.
6. The number of paths of length k between nodes i and j is given by the (i, j) th entry of \mathbf{N}^k . These paths are not necessarily distinct; that is, a path of length k going from i to j is considered distinct from an identical path going in reverse, from j to i .

Property (6) will be particularly useful. We will refer to \mathbf{N}^k as the k -th order adjacency matrix. Of particular importance will be the matrix \mathbf{N}^2 , which shows the combinations of nodes that are connected by a path of length 2, and the diagonal entries of \mathbf{N}^3 , which show the number of triangles in a directed network; multiplying the diagonal entries of \mathbf{N}^3 by a factor of 1/2 gives the number of triangles in an undirected network.

Several network metrics will be useful in decomposing systems to find embedded Wheatstone sub-networks.

Definition 1: The degree of node i , denoted d_i , is the number of edges connected to node i .

Definition 2: The distance of a path between nodes i and j is the number of edges associated with the path.

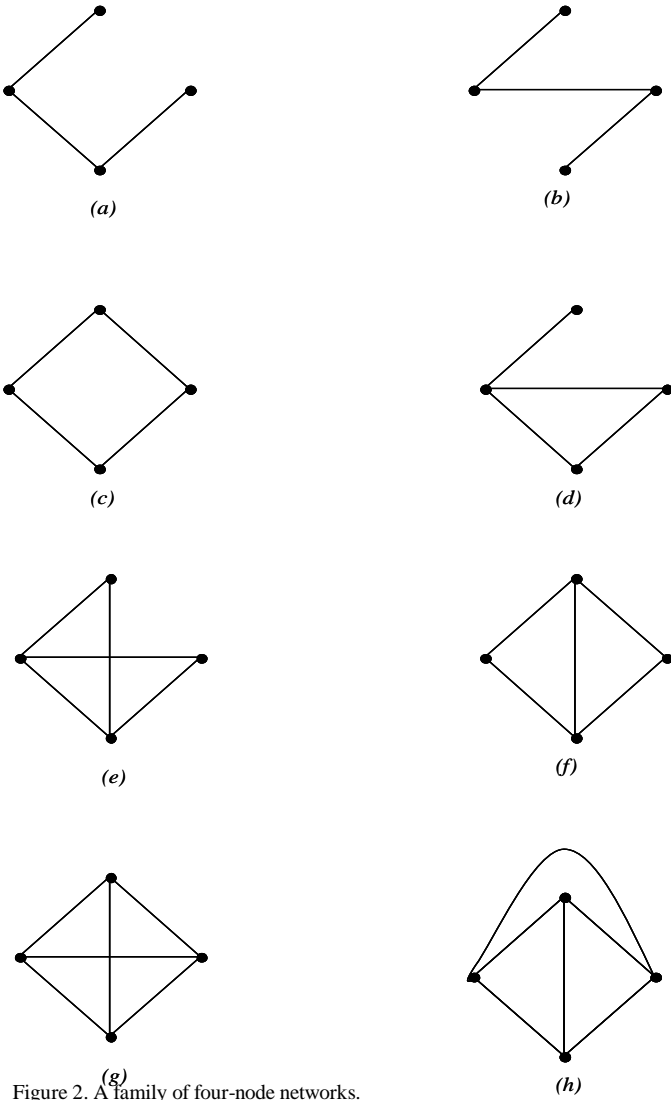


Figure 2. A family of four-node networks.

Note that the definition of distance used here is purely topological. In many situations, such as the small-world networks described by [12], this definition of distance is difficult to apply to electric power systems (a better definition would be the electrical distance between two nodes, represented by the equivalent resistance between the two nodes). For the Wheatstone-identification algorithm presented here, the canonical definition of distance will be adequate.

Definition 3: The geodesic path between nodes i and j is the minimum-distance path between nodes i and j .

The geodesic path need not be unique; in many circumstances there will be multiple geodesic paths connecting any two nodes. [13] also defines a network-wide geodesic path metric as the harmonic mean of all geodesic path lengths. The network search algorithm will only require knowing whether the geodesic path between any two nodes i and j is equal to one, two, or three. This is easily verified directly using the node-node adjacency matrix raised to the

appropriate power.

Definition 4: The local clustering metric for node i , denoted K_i , is given by the ratio of the number of triangles connected to vertex i to the number of triples centered on vertex i .¹

Nodes with only one connecting edge are given a clustering value of $K_i = 0$. The local clustering coefficient measures the proportion of possible interconnections among neighboring nodes that actually exist.

Definition 5: The network clustering metric is given by
$$K = \frac{1}{|\{i | K_i \neq 0\}|} \sum_{\{i | K_i \neq 0\}} K_i .$$
 Values of K_i equal to zero are

ignored in the computation; thus, the denominator and the limit of summation are both determined by the number of nodes having more than one connecting edge.²

Definitions (1) through (5) will help establish the following topological properties of the Wheatstone network, as shown in Figure 1.

Result 1: The network geodesic path metric for the Wheatstone network is two. The cardinality of this geodesic path metric is also two.

Proof of Result 1: The result can easily be seen by examining the Wheatstone network in Figure 1. The geodesic paths are $\{A,C,B\}$ and $\{A,D,B\}$, which traverse the boundary of the Wheatstone network.

Result 2: The Wheatstone network has a clustering metric of $K = 5/6$, where K is defined using the formulae in Definitions 4 and 5. Further, the clustering metric of the Wheatstone network is unique among four-node networks where the minimum-distance geodesic path (of all pairs of nodes) is two.

Proof of Result 2: A network where the minimum-distance geodesic path is greater than one represents a network with no atomistic nodes. Without loss of generality, the family of four-node networks meeting this qualification is shown in Figure 2.

The first part of the proof is established by calculating the clustering metric of the Wheatstone network in Figure 2(f), using Definitions 4 and 5:

¹ This definition of clustering is due to [12].

² This network clustering metric is also due to [12]. An alternative clustering metric has been proposed by [14], which measures the ratio of triangles in the network to paths of length 3 in the network, multiplied by a factor of three to account for each triangle being represented as a part of three triples [13].

$$K_{wheatstone} = \frac{1}{4} \left(1 + \frac{2}{3} + \frac{2}{3} + 1 \right) = \frac{5}{6}.$$

The remainder of the proof calculates the clustering metric for the other networks in Figure 2.

First, note that Figures 2(a) through 2(c) have no triangles, and thus have a clustering metric of zero. Also, the completely connected network in Figure 2(g) has a clustering metric of one.

The clustering metric of the network in Figure 2(d) is:

$$K_{5.3(d)} = \frac{1}{4} (1 + 1 + 1) = \frac{3}{4}.$$

The clustering metric of the network in Figure 2(e) is:

$$K_{5.3(e)} = \frac{1}{4} \left(\frac{1}{3} + 1 + \frac{2}{3} + 1 \right) = \frac{3}{4}.$$

The clustering metric of the network in Figure 2(h) is:

$$K_{5.3(h)} = \frac{1}{4} \left(\frac{2}{3} + \frac{2}{3} + \frac{2}{3} + \frac{2}{3} \right) = \frac{2}{3}.$$

Note that there is a Wheatstone network embedded in Figure 2(h). However, the link paralleling the Wheatstone sub-network reduces the minimum-distance geodesic path to one.

Result 3: Let \mathbf{N} and \mathbf{N}^2 be the first-order and second-order node-node adjacency matrices of a network, and let $\tilde{\mathbf{N}} = \mathbf{1} - \mathbf{N}$, where $\mathbf{1}$ is a matrix of ones having the same dimensions as \mathbf{N} . The pairs of nodes in the network with a geodesic path of length two correspond to the off-diagonal nonzero entries of \mathbf{N}_{g2} , where the (i,j) th entry of \mathbf{N}_{g2} is given by $N_{g2,ij} = \tilde{N}_{ij} N_{ij}$.

Proof of Result 3: This result will be useful in actually implementing the Wheatstone detection algorithm. To construct the matrix \mathbf{N}_{g2} , note that if the (i,j) th entry of \mathbf{N} is equal to one (corresponding to a geodesic path of length one between nodes i and j), then the corresponding entry of $\tilde{\mathbf{N}}$ is zero. Similarly, if the (i,j) th entry of \mathbf{N} is equal to zero, the corresponding entry of $\tilde{\mathbf{N}}$ is equal to one. To calculate \mathbf{N}_{g2} , we simply multiply the (i,j) th entry of $\tilde{\mathbf{N}}$ by the corresponding entry of \mathbf{N}^2 . Entries of \mathbf{N}_{g2} can be equal to zero if the corresponding entry of $\tilde{\mathbf{N}}$ is equal to zero or if the corresponding entry of \mathbf{N}^2 is equal to zero (or both). Nonzero off-diagonal entries of \mathbf{N}_{g2} correspond to pairs of nodes whose geodesic path is equal to two.

III. DETECTING EMBEDDED WHEATSTONE NETWORKS

One goal of the Wheatstone detection algorithm is to disqualify certain nodes, paths, or pairs of nodes from possibly being part of a Wheatstone sub-network. The matrices \mathbf{A} , \mathbf{N}^2 and \mathbf{N}^3 will be particularly useful for this purpose. The graph-theoretic preliminaries in Section II give us the following exclusion principles:

1. Any node having degree one cannot be part of a Wheatstone sub-network. This can be verified using the node-line adjacency matrix \mathbf{A} . If the i th row of \mathbf{A} has at most one non-zero entry, then the degree of node i is equal to one. This property can also be verified using \mathbf{N} . If the i th row or column of \mathbf{N} sums to exactly one, then node i has degree one.
2. For any pair of nodes i and j , if there is no path of length two or three connecting i and j , then that pair of nodes cannot be part of a Wheatstone network. This property can be verified by looking at the i, j th entry of \mathbf{N}^2 and \mathbf{N}^3 .
3. If there are no triangles attached to the i th node, then that node cannot be part of a Wheatstone network. The diagonal entries of \mathbf{N}^3 can verify this property.

Nodes that are connected simply in series or parallel within larger Wheatstone networks would result in violations of the Wheatstone criteria. The algorithm would thus return a “false negative” for these types of sub-networks, failing to identify an embedded Wheatstone sub-network. Simple series and parallel connections will need to be compressed into single edges or nodes in order to avoid false negatives. Note that the algorithm will create equivalent series-parallel nodes and edges only in a topological sense. Once the Wheatstone networks in the larger system have been identified, the electrical topology of the entire system will be preserved in order to analyze the Wheatstones.

The Wheatstone detection algorithm proceeds as follows:

Step 1: Calculate the node-node adjacency matrices \mathbf{N} , \mathbf{N}^2 and \mathbf{N}^3 for the network, as well as the node-edge adjacency matrix \mathbf{A} .

Step 2: Compress all simple series and parallel connections into single equivalent nodes or edges. Simple parallel connections can be detected easily using the \mathbf{A} matrix; two edges are parallel if their corresponding columns in the \mathbf{A} matrix are equal. Two edges connected in series can be detected by noting that the node connecting them has degree two and is not connected to any triangles [10]. The degree of each node can be calculated using the \mathbf{A} matrix, while the number of triangles connected to each node can be read from the diagonal entries of \mathbf{N}^3 . More than one iteration of this step may be required.

Step 3: Define T as the set of nodes that are part of at least one triangle.

Step 4: Define D as the set of nodes that have degree greater than one.

Step 5: Define R_1 as the set of all pairs of nodes that have geodesic path length equal to two. Define R_2 as the set of all pairs of nodes that have geodesic path length equal to two and also have two geodesic paths. Thus, $R_2 \subset R_1$. Note the strategy behind the definitions of R_1 and R_2 ; the aim is to determine whether a given pair of nodes might represent the endpoints of an embedded Wheatstone sub-network (as in Figure 5.2). Define R_3 as the set of all pairs of nodes connected by exactly two paths of length three.

Step 6: Define $WS = T \cap D \cap R_2 \cap R_3$. Some care is required in defining the intersection of these sets, since T and D contain a list of nodes, whereas R_2 and R_3 contain a list of pairs of nodes. If Ω is a set of single elements, and Ψ is a set of pairs of elements, then we will say that $\{\psi_i, \psi_j\} \in \Omega \cap \Psi$ if and only if $\psi_i \in \Omega$ and $\psi_j \in \Omega$, for all $\psi_i, \psi_j \in \Psi$.

WS represents pairs of nodes that meet the necessary conditions for being part of a Wheatstone network; Steps 7 and 8 will determine whether the nodes in WS also meet the sufficiency conditions.

Step 7: For all pairs of nodes $\{(i,j)\}$ in WS , construct the node-node adjacency matrix for the subgraph consisting of i , j , and all nodes that are neighbors of both i and j (that is, those nodes which have a geodesic path distance of one from both i and j). Ignore any direct links between i and j .

Step 8: Calculate the clustering coefficient for all the subgraphs generated in Step 7. Those for which $K = 5/6$ represent Wheatstone sub-networks.

The network decomposition algorithm will be illustrated with a simple example.

IV. ILLUSTRATING THE WHEATSTONE DETECTION ALGORITHM

The thirteen-bus network shown in Figure 2 is used to illustrate how the algorithm identifies Wheatstone sub-networks. The network is based on the topology of the IEEE fourteen-bus test case, but has been altered by removing all of the synchronous condensers and winding transformers from the system, which reduces the size to thirteen buses and alters the network topology.

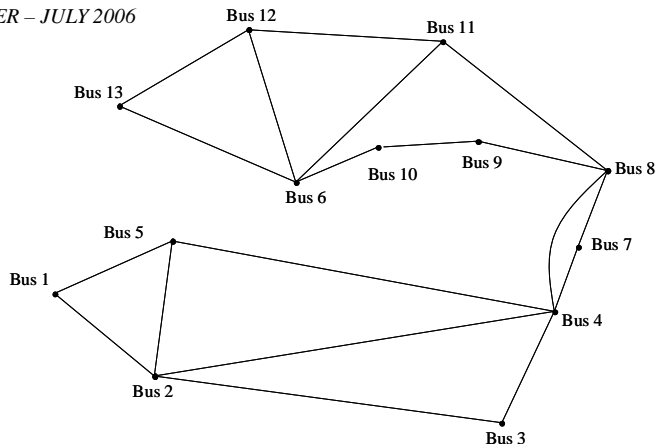


Figure 2. Topological representation of the thirteen-bus test network used to illustrate the Wheatstone detection algorithm. The network is based on the IEEE fourteen-bus network, but the synchronous condensers and winding transformers have been removed.

The first step in the algorithm is to calculate the node-line adjacency matrix \mathbf{A} ; this matrix is contained in the Appendix. From the node-edge incidence matrix, we see that nodes 6, 8, 9, and 10 are all connected in series; thus, for topological purposes, we can compress this group into a single line connecting nodes 6 and 8. Similarly, nodes 4 and 8 have a simple series-parallel connection; thus, we can also eliminate bus 7. This reduces the network down to ten nodes and fifteen lines.

The node-node adjacency matrices \mathbf{N} , \mathbf{N}^2 and \mathbf{N}^3 for the reduced network are calculated next; these are also shown in the Appendix. The number of triangles associated with each node is given by the diagonals of \mathbf{N}^3 multiplied by a factor of 0.5. It will be useful to define a matrix $\mathbf{T} = \frac{1}{2} \text{diag}(\mathbf{N})$, whose i th diagonal entry shows the number of distinct triangles connected to the i th node in the network. All off-diagonal entries of \mathbf{T} are equal to zero.

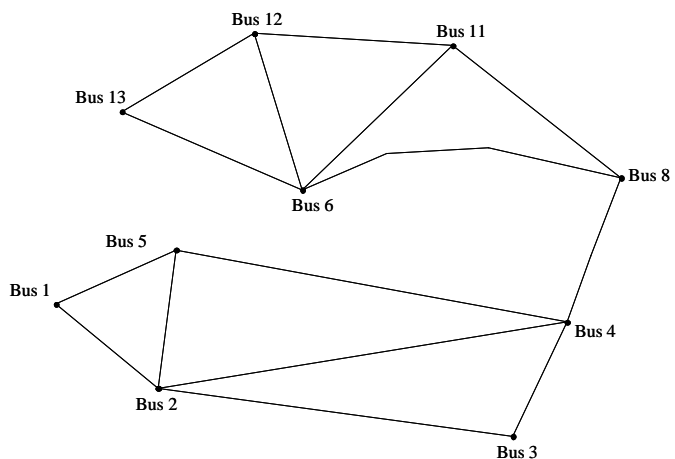


Figure 3. The reduced-form thirteen-bus network, after creating equivalent series-parallel connections in the system.

Following the series-parallel reduction in Steps 1 and 2 of the decomposition algorithm, we obtain the reduced form of the thirteen-bus network, shown in Figure 3.

In step 4 we find the set of all nodes with degree greater

than one. Recall that the degree of a node is equal to the number of connected neighbors – that is, the number of nodes to which each node is directly connected. The degree of each node can be found in two different ways. The first method uses the node-line adjacency matrix; the degree of each node is equal to the sum of the absolute values of the entries in the corresponding row of the node-line incidence matrix. The second method uses the node-node adjacency matrix. The degree of a given node is equal to the sum of the corresponding row or column in the node-node adjacency matrix. Thus, we have:

Method 1: $d_i = \sum_j |a_{ij}|$, or

Method 2: $d_i = \sum_j N_{ij} = \sum_j N_{ji}$.

Figure 4 illustrates the calculation using method 2; the figure shows the reduced network node-node adjacency matrix plus an extra column summing the entries in each row.

From Figure 5.12, we see that every node in the reduced network has degree greater than one. Thus, the set D contains every node in the network (note also that D is equal to the set T of all nodes connected to at least one distinct triangle):

$$D = \{1, 2, 3, 4, 5, 6, 8, 11, 12, 13\}.$$

Step 5 requires that we determine the membership of three sets, labeled R_1 , R_2 , and R_3 . The set R_1 is made up of all pairs of nodes with geodesic path length equal to two. R_2 is made up of the subset of R_1 consisting of all pairs of nodes whose geodesic path length is equal to two, and for which the cardinality of the geodesic path is also two (that is, the pairs of nodes for which there are two geodesic paths). R_3 is the set of all pairs of nodes that are separated by two paths of length three. This set is not a subset of either R_1 or R_2 , but is grouped with R_1 and R_2 since its members can be determined in parallel with R_1 and R_2 .

											Degree	
$N =$	0	1	0	0	1	0	0	0	0	0	0	2
	1	0	1	1	1	0	0	0	0	0	0	4
	0	1	0	1	0	0	0	0	0	0	0	2
	0	1	1	0	1	0	1	0	0	0	0	4
	1	1	0	1	0	0	0	0	0	0	0	3
	0	0	0	0	0	0	1	1	1	1	1	4
	0	0	0	1	0	1	0	1	0	0	0	3
	0	0	0	0	0	0	1	1	0	1	0	3
	0	0	0	0	0	0	1	0	1	0	1	3
	0	0	0	0	0	0	1	0	0	1	0	2

Figure 4. The degree of all ten nodes in the reduced-form network.

To determine which nodes are members of R_1 , R_2 , and R_3 , we use Result 3 to calculate the matrix N_{g2} , which is shown in Figure 5.

$$N_{g2} = \begin{bmatrix} 2 & 0 & 1 & 2 & 0 & 0 & 0 & 0 & 0 & 0 \\ 0 & 4 & 0 & 0 & 0 & 0 & 1 & 0 & 0 & 0 \\ 1 & 0 & 2 & 0 & 2 & 0 & 1 & 0 & 0 & 0 \\ 2 & 0 & 0 & 4 & 0 & 1 & 0 & 1 & 0 & 0 \\ 0 & 0 & 2 & 0 & 3 & 0 & 1 & 0 & 0 & 0 \\ 0 & 0 & 0 & 1 & 0 & 4 & 0 & 0 & 0 & 0 \\ 0 & 1 & 1 & 0 & 1 & 0 & 3 & 0 & 2 & 1 \\ 0 & 0 & 0 & 1 & 0 & 0 & 0 & 3 & 0 & 2 \\ 0 & 0 & 0 & 0 & 0 & 0 & 2 & 0 & 3 & 0 \\ 0 & 0 & 0 & 0 & 0 & 0 & 1 & 2 & 0 & 2 \end{bmatrix}$$

Figure 5. The off-diagonal entries of the matrix N_{g2} show the pairs of nodes with geodesic path length equal to two.

Reading off the nonzero off-diagonal entries from Figure 5 yields the set R_1 :

$$R_1 = \{\{1,3\}, \{1,4\}, \{2,8\}, \{3,5\}, \{3,8\}, \{4,6\}, \{4,11\}, \{5,8\}, \{8,12\}, \{8,13\}, \{11,13\}\}.$$

Since N^2 contains all paths of length two between pairs of nodes in the network, and since N_{g2} indicates which pairs of nodes have a geodesic path length equal to two, those entries of N_{g2} equal to two indicate which pairs of nodes have exactly two geodesic paths. These pairs of nodes form the set R_2 . Figure 5.13 allows us to identify the set R_2 :

$$R_2 = \{\{1,4\}, \{3,5\}, \{8,12\}, \{11,13\}\}.$$

To complete step 5 of the Wheatstone detection algorithm, we must find the set R_3 . Since we are looking for pairs of nodes that are separated by at least two paths of length three, we need only look at the entries of N^3 . For a reasonably meshed network, R_3 will be quite large; for the reduced network shown in Figure 5.11, we get:

$$R_3 = \{\{1,2\}, \{1,3\}, \{1,4\}, \{1,5\}, \{1,8\}, \{2,3\}, \{2,4\}, \{2,5\}, \{2,8\}, \{3,4\}, \{3,5\}, \{4,5\}, \{4,8\}, \{4,12\}, \{6,8\}, \{6,11\}, \{6,12\}, \{6,13\}, \{8,11\}, \{8,12\}, \{8,13\}, \{11,12\}, \{11,13\}, \{12,13\}\}.$$

The set $R_2 \cap R_3$ consists of pairs of nodes that might represent the endpoints of a Wheatstone sub-network (these correspond to nodes A and B in Figure 1), and in this case, $R_2 \cap R_3 = R_2$ since $R_2 \subset R_3$. Thus, from Figure 5, we see that there are at most four Wheatstone sub-networks in the reduced network shown in Figure 3.

Step 6 of the Wheatstone detection algorithm requires that we calculate the set WS , defined as the intersection of T , D , R_2 , and R_3 . To handle calculating the intersection of two sets, the first of which contains a list of nodes, and the second of which contains a set of pairs of nodes, we will require that both members of each pair of nodes in the second set also individually be members of the first set. Since both T and D contain all the nodes in the reduced network, and $R_2 \cap R_3 = R_2$, we see that $WS = R_2$.

In step 7 of the Wheatstone detection algorithm, we construct the sub-graphs consisting of pairs of nodes $\{i,j\}$ in

the set WS and all nodes connected to both i and j with degree one. Step 8 verifies that these are indeed Wheatstone sub-networks by calculating the clustering coefficient of each sub-graph. Since there are four pairs of nodes in the set WS , we must construct four distinct sub-graphs.

The set of nodes connected to both i and j with degree one can be found by scanning the i th and j th column (or row) of the node-node adjacency matrix \mathbf{N} , looking for common elements whose entry is equal to one:

$$\{\text{nodes connected to } i \text{ and } j \text{ with degree one}\} = \{k \mid N_{ik} = 1\} \cap \{k \mid N_{jk} = 1\}, k = 1, \dots, NB.$$

$$\begin{aligned} \mathbf{WS}_1 &= \begin{matrix} 1 & 2 & 4 & 5 \\ 2 & 1 & 0 & 1 \\ 4 & 0 & 1 & 1 \\ 5 & 1 & 1 & 0 \end{matrix} & \mathbf{WS}_3 &= \begin{matrix} 6 & 8 & 11 & 12 \\ 6 & 1 & 1 & 1 \\ 8 & 1 & 0 & 0 \\ 11 & 0 & 1 & 1 \\ 12 & 1 & 0 & 0 \end{matrix} \\ \mathbf{WS}_2 &= \begin{matrix} 2 & 3 & 4 & 5 \\ 2 & 1 & 1 & 1 \\ 3 & 1 & 0 & 0 \\ 4 & 1 & 1 & 1 \\ 5 & 1 & 0 & 0 \end{matrix} & \mathbf{WS}_4 &= \begin{matrix} 6 & 11 & 12 & 13 \\ 6 & 1 & 1 & 1 \\ 11 & 1 & 0 & 1 \\ 12 & 1 & 1 & 0 \\ 13 & 1 & 0 & 0 \end{matrix} \end{aligned}$$

Figure 6. The node-node adjacency matrices for the four candidate Wheatstone sub-networks of the ten-bus reduced network.

The node-node adjacency matrices for the four candidate Wheatstone sub-networks of the reduced network shown in Figure 3 are shown in Figure 6. Using the clustering metric given in Definition 5, we see that $K = 5/6$ for all four candidate Wheatstone sub-networks in Figure 6. Thus, all four are actual Wheatstone sub-networks.

V. STEADY-STATE ANALYSIS OF EMBEDDED WHEATSTONE NETWORKS

Once identified, the steady-state properties of power flow through Wheatstone sub-networks can be identified. Blumsack and Ilić analyze a four-bus Wheatstone test network in the steady state. They derive the conditions under which the addition of a Wheatstone bridge will cause congestion in the network (the Braess Paradox), and the conditions under which the network will display the following phenomena of interest for congestion management and transmission planning:

1. Local network upgrades will not relieve congestion; capacity limits must be increased throughout the network or the Wheatstone bridge must be removed to get rid of congestion.
2. The Wheatstone bridge causes congestion, but may increase the reliability of the system (Blumsack, Lave, and Ilić 2006).
3. The nodal prices and shadow prices of transmission may identify the presence of network congestion, but do not necessarily identify the best way to relieve that congestion.

Wheatstone sub-networks embedded in larger systems can be analyzed in much the same way as the four-bus test network, but care must be taken to incorporate the effects of

the external network. This requires creating two distinct types of equivalent buses and lines in the network. The first equivalencing method uses the delta-star formulas to collapse series-parallel connections into single equivalent network structures. This is the electrical equivalent of the series-parallel concatenation in Step 1 of the network decomposition algorithm presented in Section 4.

The second equivalencing method required uses the information in the external network to create equivalent flows between the external network and the embedded Wheatstone sub-network of interest. Several methods exist for calculating equivalent steady state flows; we illustrate using the Ward equivalent. The methods are not perfect. The Ward equivalent in particular has two well-known drawbacks. The first is that while it replicates real power flows reasonably well [15], it is less accurate in reproducing the full-network reactive flows. The second is that it assumes that the external network is in a static steady state. Thus, injections, withdrawals, line impedances, and so forth do not deviate from their constant steady-state values. Thus, the equivalencing methods are most useful for examining the effects of small changes in the network.

Derivation of the Ward equivalent is described in detail in [16] and [15]. We provide only a brief outline here. The primary tool in the Ward equivalent method is the system admittance matrix \mathbf{Y} (or, in the case of the DC power flow, the system susceptance matrix \mathbf{B}), which is partitioned according to the number of nodes in each of the internal, external, and boundary subsystems. If there are e nodes in the external system, i nodes in the internal system, and b nodes on the boundary, then we define the following partitions of the \mathbf{Y} matrix:³

\mathbf{Y}_{EE} = the $(e \times e)$ sub-matrix of admittances in the external system;

\mathbf{Y}_{BE} = the $(b \times e)$ sub-matrix of admittances between the boundary nodes and the external system;

\mathbf{Y}_{BI} = the $(b \times i)$ sub-matrix of admittances between the boundary nodes and the internal nodes;

\mathbf{Y}_{II} = the $(i \times i)$ sub-matrix of admittances in the internal system.

The full system admittance matrix is thus partitioned as follows:

$$\mathbf{Y}_{\text{system}} = \begin{bmatrix} \mathbf{Y}_{EE} & \mathbf{Y}_{EB} & \mathbf{0} \\ \mathbf{Y}_{BE} & \mathbf{Y}_{BB}^E + \mathbf{Y}_{BB}^I & \mathbf{Y}_{BI} \\ \mathbf{0} & \mathbf{Y}_{IB} & \mathbf{Y}_{II} \end{bmatrix}.$$

Note that $\mathbf{Y}_{BE} = \mathbf{Y}_{EB}^T$ and $\mathbf{Y}_{BI} = \mathbf{Y}_{IB}^T$. The submatrices \mathbf{Y}_{BB}^E and \mathbf{Y}_{BB}^I contain the sum of admittances between the boundary buses and the external and internal buses,

³ Note that $e + i + b = NB$, the number of buses in the network.

respectively. The part of the $\mathbf{Y}_{\text{system}}$ matrix describing the external system can be divorced from the part representing the internal system, as:

$$\mathbf{Y}_E = \begin{bmatrix} \mathbf{Y}_{EE} & \mathbf{Y}_{EB} \\ \mathbf{Y}_{BE} & \mathbf{Y}_{BB}^E \end{bmatrix}.$$

Through repeated application of Ohm's Law for the external, internal, and boundary systems, the external equivalent admittance matrix is:

$$\mathbf{Y}_{\text{eq}} = \mathbf{Y}_{BB}^E - \mathbf{Y}_{BE} \mathbf{Y}_{EE}^{-1} \mathbf{Y}_{EB}.$$

Here, we demonstrate the equivalencing steady-state analysis method using the 13-bus network from Section 4. The equivalent reduced network has ten buses; buses 7, 9, and 10 are eliminated in series. Thus, the reduced admittance matrix is a (10×10) matrix of equivalent admittances. The example presented here will focus on the four-bus Wheatstone network consisting of buses 6, 11, 12, and 13. For simplicity, we will invoke the usual DC power flow assumptions and consider only the reactive portion of the full network admittance matrix.

The Ward equivalent susceptance matrices for the reduced-form network are shown in Figure 7. The internal buses for the Ward calculation are buses 12 and 13 (not all four buses of the Wheatstone network, since the Ward equivalent technique makes a distinction between the internal and boundary buses). Referencing Figure 3, the boundary buses are buses 6 and 11. The external buses consist of the remainder of the network.

$$\mathbf{B}_{II} = \begin{bmatrix} 4.04 & 7.35 \\ 7.35 & 18 \end{bmatrix}$$

$$\mathbf{B}_{BI} = \begin{bmatrix} -6.21 & -11.3 \\ 0.76 & -3.49 \end{bmatrix}$$

$$\mathbf{B}_{BE} = \begin{bmatrix} 1.45 & -2.59 & -3.78 & 3.05 & 0.71 & 4.37 \\ -1.47 & 2.63 & 3.84 & -3.09 & -0.72 & -0.54 \end{bmatrix}$$

$$\mathbf{B}_{EE} = \begin{bmatrix} 0.46 & -0.82 & -1.2 & 0.97 & 0.22 & 0.66 \\ -0.82 & 1.47 & 2.15 & -1.73 & -0.4 & -1.18 \\ -1.2 & 2.15 & 3.14 & -2.53 & -0.59 & -1.73 \\ 0.97 & -1.73 & -2.53 & 2.04 & 0.47 & 1.39 \\ 0.22 & -0.4 & -0.59 & 0.47 & 0.11 & 0.32 \\ 0.66 & -1.18 & -1.73 & 1.39 & 0.32 & 2 \end{bmatrix}$$

Figure 7. The Ward equivalent matrices for the reduced-form thirteen-bus network.

The Ward equivalent external susceptance matrix is given by:

$$\mathbf{B}_{E,\text{eq}} = \begin{bmatrix} -13.61 & 2.04 \\ -0.53 & -5.98 \end{bmatrix}.$$

Thus, the Ward equivalent susceptance matrix for the Wheatstone subnetwork is:

$$\mathbf{B}_{I,\text{eq}} = \begin{bmatrix} -13.61 & 2.04 & -6.21 & 0.76 \\ -0.53 & -5.98 & -11.3 & -3.49 \\ -6.21 & -11.3 & 4.04 & 7.35 \\ 0.76 & -3.49 & 7.35 & 48 \end{bmatrix}.$$

The information in the equivalent susceptance matrix can be combined with the topological information from the Wheatstone network in order to characterize the injections or withdrawals at the boundary buses, as well as the flows through the network. Figure 8(a) shows the Wheatstone subnetwork without the additional information from the equivalent external system and Figure 8(b) shows the Wheatstone following the equivalencing procedure. Note that the direction of flows through the network is not altered by the Ward equivalent.

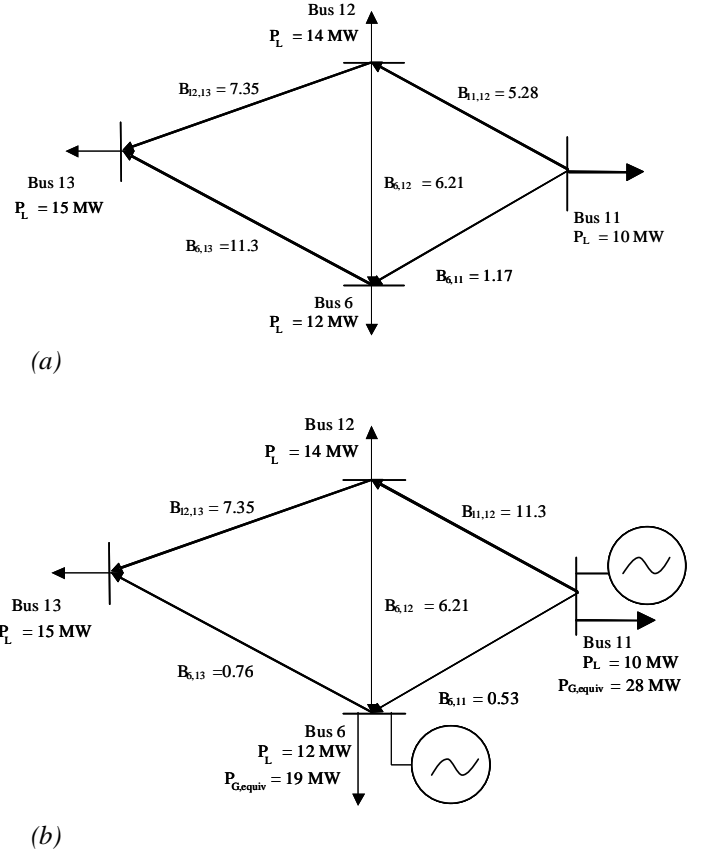


Figure 8. The original Wheatstone sub-network is shown in panel (a), while the equivalent sub-network formed using the Ward equivalent is shown in panel (b).

VI. CONCLUSION

Previous research has demonstrated that the presence of a

Wheatstone sub-network in a larger power system may cause some unexpected effects, such as congestion that is not relieved with incremental upgrades. The pricing signals in Wheatstone sub-networks may also be misleading. However, the Wheatstone structure may simultaneously offer a reliability benefit to the system. While this behavior is easy to analyze in the context of a simple four-bus Wheatstone model system, it may be harder to pin down in a large meshed network. Being able to find embedded Wheatstone structures is valuable in both the operations and planning functions of grid management.

This paper has developed a graph-theoretic network search tool to find Wheatstone sub-networks in larger systems. The search tool is heuristic in the sense that it does not perform a complete combinatorial scan of all possible four-node sub-networks. For even modestly-sized systems, the combinatorial problem is too large. Instead the search algorithm exploits the unique graph-theoretic structure of the Wheatstone network. The tool was illustrated on a modified version of the IEEE fourteen-bus network; this network was chosen in order to provide a sufficiently interesting example where the outcome could also be seen though a simple visual scan of the network. The paper also illustrated the use of creating equivalent network structures to incorporate the power grid's electrical properties into the Wheatstone search algorithm, and to facilitate the analysis of individual embedded Wheatstone sub-networks.

VII. ACKNOWLEDGMENTS

The author would like to thank Lester Lave, Marija Ilic, William Hogan, Paul Hines, Jose Moura, and Sarosh Talukdar for helpful comments and discussions.

VIII. REFERENCES

- [1] Blumsack, S., 2006. *Network Topologies and Transmission Investment Under Electric-Industry Restructuring*, Ph.D. dissertation, Department of Engineering and Public Policy, Carnegie Mellon University, available at <http://wpweb2k.gsia.cmu.edu/ceic/phd.htm#Blumsack>.
- [2] Blumsack, S. and M. Ilić, 2006. "The Braess Paradox in Electric Power Networks," working paper.
- [3] Braess, D., 1968. "Über ein Paradoxon aus der Verkehrsplanung," *Unternehmensforschung* 12, pp. 258 – 268.
- [4] Cohen, J. and P. Horowitz, 1991. "Paradoxical Behavior of Mechanical and Electrical Networks," *Nature* 352, pp. 699 – 701.
- [5] Calvert, B. and G. Keady, 1993. "Braess' Paradox and Power Law Nonlinearities in Networks," *Journal of the Australian Mathematical Society B* 35, pp. 1 – 22.
- [6] Korilis, Y., Lazar, A., and A. Orda, 1999. "Avoiding the Braess Paradox in Non-Cooperative Networks," *Journal of Applied Probability* 36, pp. 211 – 222.
- [7] Blumsack, S., L. B. Lave, and M. Ilić, 2006. "The Relationship Between Congestion and Reliability," working paper.
- [8] Kron, G., 1953. "A Set of Principles to Interconnect the Solutions of Physical Systems," *Journal of Applied Physics* 24:8, pp. 965 – 980.
- [9] Happ, H., 1974. "Diakoptics: The Solution of System Problems by Tearing," *Proceedings of the IEEE* 62:7, pp. 930 – 940.
- [10] Duffin, R., 1965. "Topology of Series-Parallel Networks," *Journal of Mathematical Analysis and Applications* 10, pp. 303 – 318.
- [11] Milchtaich, I., 2005. "Network Topology and Efficiency of Equilibrium," Bar-Ilan University Department of Economics Working Paper.
- [12] Watts, D. and H. Strogatz, 1998. "Collective Dynamics of 'Small-World' Networks," *Nature* 393, pp. 440 – 442.

- [13] Newman, M. E. J., 2003. "The Structure and Function of Complex Networks," *SIAM Review* 45:2, pp. 167 – 256.
- [14] Barrat, A. and M. Weigt, 2000. "On the Properties of Small-World Networks," *European Journal of Physics B* 13, pp. 547 – 560.
- [15] Lo, K., L. Peng, J. Macqueen, A. Ekwue, and N. Dandachi, 1993. "Extended Ward Equivalent of External System for On-Line Security Analysis," *Proceedings of the IEEE 2nd International Conference on Advances in Power System Control*, Hong Kong.
- [16] Monticelli, A., S. Deckmann, A. Garcia, and B. Stott, 1979. "Real-time External Equivalents for Static Security Analysis," *IEEE Transactions on Power Apparatus and Systems* PAS-98, pp. 498 – 508.